JOURNAL OF MATERIALS SCIENCE **36** (2001) 3215–3220

Surface effects in chromate conversion coatings on 2024-T3 aluminum alloy

X. SUN, R. LI, K. C. WONG, K. A. R MITCHELL
Department of Chemistry, University of British Columbia, 2036 Main Mall, Vancouver, British Columbia, Canada V6T 1Z1
E-mail: karm@chem.ubc.ca

T. FOSTER
Dockyard Laboratory (Pacific), Defence Research Establishment Atlantic, PO Box 17000 STN Forces, Victoria, British Columbia, Canada V9A 7N2

Chromate conversion coatings formed on samples of 2024-T3 aluminum alloy, which had been given different pre-treatments, were examined by transmission electron microscopy (TEM), X-ray photoelectron spectroscopy (XPS), scanning electron microscopy (SEM) and corrosion tests. Two pre-treatments were considered, namely a simple mechanical polish, and polishing followed by an etch in a HF-H_2SO_4 solution. The latter treatment leads to significant Cu enrichment at the oxide-alloy interface, and this in turn can lead to a deleterious effect on the corrosion protection afforded by a subsequently applied chromate coating. Discussions are given of the behaviour of Cu in the coating formed on the sample that received an acid etch in the pre-treatment. This involves both migration through the coating and a non-uniform redeposition of Cu on to the coating surface. By contrast, the sample that initially was given just the mechanical polish in the pre-treatment does not show a Cu enrichment in the surface region, and the subsequently applied coating appeared stable after a 24 h immersion in a NaCl test solution.

1. Introduction

Conversion coatings formed on aluminum and its alloys, by treating in chromate-fluoride baths, have found extensive industrial applications as a result of their abilities to provide improved corrosion resistance, in part through their suitability for the adhesive application of paints and other organic layers [1]. These uses have more recently been overshadowed by the environmental problems associated with the use of chromate, and hence a substantial effort is underway to find new, effective and environmentally-benign protective coatings [2].

Extensive studies have been made of the structure and composition of conversion coatings on aluminum using various analysis techniques including X-ray photoelectron spectroscopy (XPS) [3–5], Auger electron spectroscopy (AES) [6, 7], secondary ion mass spectrometry (SIMS) [8], Rutherford backscattering spectroscopy (RBS) [9], Fourier transform infrared spectroscopy (FTIR) [10], X-ray absorption spectroscopy (XAS) [10, 11] and transmission electron microscopy (TEM) [12–14]. These studies have provided an increased understanding of the coating process, particularly on pure aluminum, but it is also recognized that alloying elements can modify mechanistic effects at various stages associated with coating formation [1]. Aluminum alloys that contain copper are industrially important, such as in aerospace applications, but the study of Cu interfacial enrichment has focused mainly on model alloys [15, 16] and on thin film alloys [17, 18] involving treatments such as anodizing [17], chemical polishing [15], electropolishing [16] or alkaline etching [19]. For conversion coatings formed on commercial alloys of this type, very little attention has been given to Cu enrichment and its role in the coating, although an initial study for phosphating Al-2024 alloy showed that Cu enrichment can have a marked effect on the process [20].

The development of new coating procedures would be helped by having a better understanding of the chromating process, particularly because it provides a basic reference through which the alternatives may be assessed. In this regard, the present work aims to examine Cu enrichments at alloy-to-oxide interfaces resulting from different pre-treatments, as well as the involvement of this Cu in the subsequent chromating processes, including the performances of these coatings for corrosion inhibition. This research characterizes chromate coatings formed on Al-2024 alloy especially by TEM, XPS, scanning electron microscopy (SEM) and corrosion tests.

2. Experimental procedures

All experiments in this study used square samples (1×1 cm^2) of commercial 2024-T3 aluminum alloy which were mechanically polished by Al_2O_3-sandpaper and diamond paste (1 μm), and then ultrasonically cleaned in ethanol and methanol. Prior to a conversion coating treatment, some mechanically-polished specimens were given an acid etch for 30 s in a solution composed of 1.5 mL HF (20%), 10 mL H_2SO_4 (98%) and 90 mL H_2O. This was followed by a thorough rinse in deionized water and drying in air. All chromate-conversion treatments were carried out by immersing the samples for 5 min in the coating bath (composition 4 g CrO_3, 3.5 g $Na_2Cr_2O_7$ and 0.8 g NaF per L aqueous solution) at 298 K; this was followed by washing in deionized water and air drying.

XPS spectra were measured in a fully-equipped Leybold MAX200 system [21] with the pass energy set at 96 eV. Binding energies were referenced to C 1s structure for adventitious carbon at 285.0 eV. Depth profiling was achieved using Ar^+ sputtering for conditions (4 keV, 3 mA emission current) that gave an average etching rate of about 1.4 nm min^{-1} (this was estimated by comparing film thickness information from TEM with sputter rate information observed in the XPS depth profiles). Specimens for studying with TEM were prepared by using an ultramicrotome following standard procedures [22]. Briefly, encapsulated samples were trimmed initially with a glass knife, and sections (15–20 nm thick) were cut with a diamond knife approximately parallel to the coating-metal interface. Such samples were examined in a Phillips 300 TEM operated at 80 kV.

Electrochemical polarization measurements were conducted in a 3.5% NaCl solution using a Solartron 1286 potentiostat with corrware and corrview software for analysis. These experiments used a conventional three-electrode cell at 20°C with a potential range -1.25 to -0.5 V and a scan rate of 0.5 mVs^{-1}. Corrosion effects were assessed also by characterizing the samples after immersing in the 3.5% NaCl solution for 24 h at 20°C. This involved taking SEM images with a Hitachi S-2300 model microscope operated at 14 kV.

3. Results

3.1. Characterization of pre-treated surfaces

Fig. 1 shows a TEM micrograph measured from an ultramicrotomed section of Al-2024 alloy following a 30 s etch in the HF-H_2SO_4 solution. It is apparent that neither the alloy-to-oxide interface nor the uppermost surface are flat; also, a dark band about 3 nm thick is seen at the interface between the alloy and oxide film. The darker appearance of the band is suggestive of enhanced electron scattering from this material compared with that from Al in the alloy.

XPS measurements provide further insight into this situation. Fig. 2 compares Cu 2p spectra measured from the mechanically-polished and acid-etched Al-2024 alloy surfaces, and it is clear that much more Cu is formed at the latter surface compared with the former (the increase is approximately 40-fold). The Cu $2p_{3/2}$ binding energy of 932.4 eV observed from the acid-etched

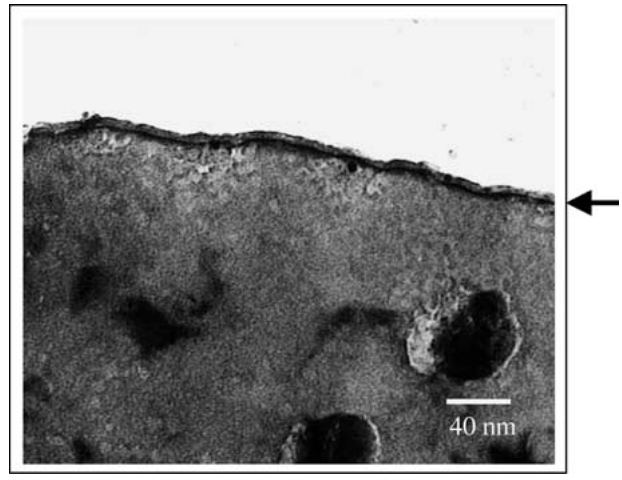

Figure 1 TEM micrograph of ultramicrotomed section of Al-2024 alloy following 30 s acid etch treatment. The arrow marks the dark band interpreted as associated with Cu enrichment at the alloy-oxide interface.

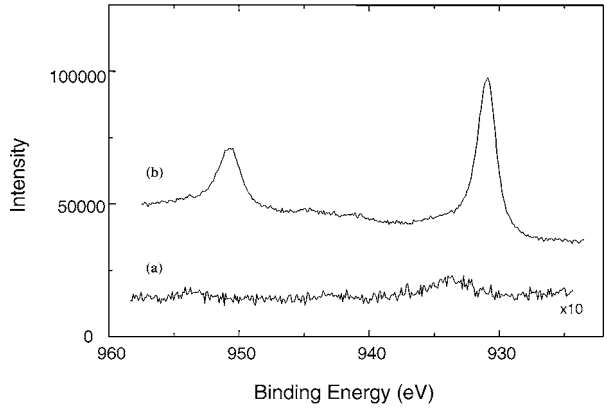

Figure 2 Cu 2p spectra measured from samples of Al-2024 alloy after (a) mechanical polishing, and (b) a subsequent 30 s etch in HF-H_2SO_4 solution.

sample is consistent with the Cu being in the metallic or slightly oxidized forms (e.g. up to Cu_2O) [23]. With these observations, it is considered highly probable that the dark band seen in the TEM micrograph from the acid-etched sample results from Cu enrichment at the alloy-oxide interface.

3.2. Comparison of chromate conversion coatings

3.2.1. TEM analysis

Fig. 3 shows TEM micrographs of ultramicrotomed sections of Al-2024 specimens following formation of a chromate conversion coating on both the mechanically-polished and acid-etched surfaces. Both chromate coatings are about 85 nm thick, although they do show differences. For example, the coating formed on the sample which just received a mechanical polish in the pre-treatment was broken during many examples of sectioning, whereas that was not the case for the coating formed on the sample which also received the acid etch. A dark band, about 3 nm thick, is revealed at the alloy-to-chromate interface for the sample that was etched, although no such band is observed for the sample that just received the mechanical polish in the pre-treatment.

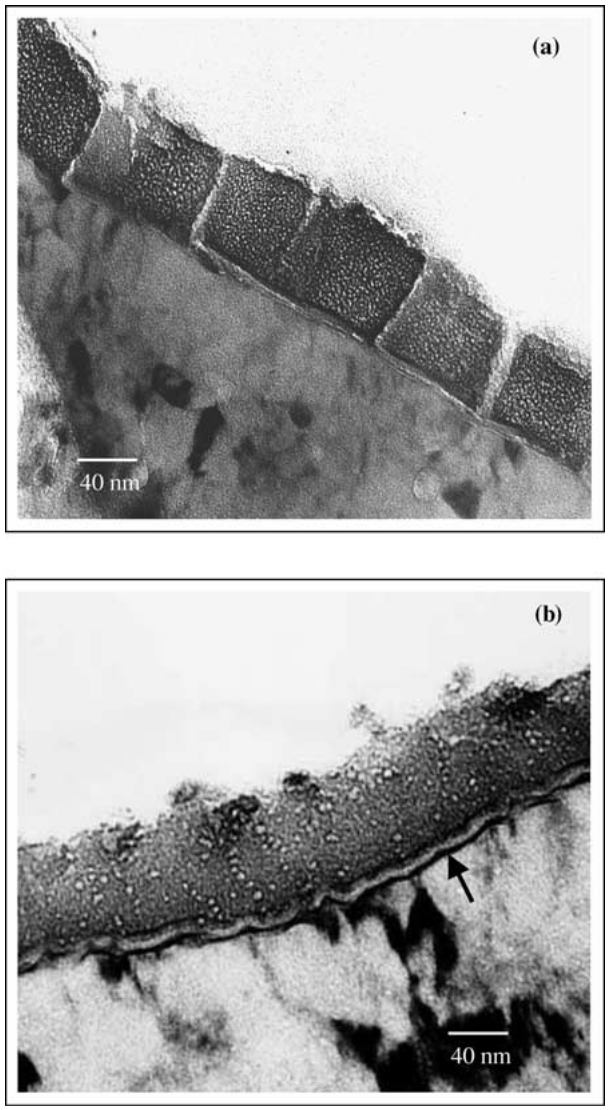

Figure 3 TEM micrographs of ultramicrotomed sections through chromate conversion coatings formed on Al-2024 samples after different pre-treatments: (a) mechanical polish only, and (b) subsequent 30 s etch in HF-H_2SO_4 solution. For (b), the arrow marks the dark band that is believed to relate to Cu enrichment at the alloy-coating interface.

The latter surface appears relatively flat, while the top surface from the sample which received the acid etch shows a rougher coating with local protrusions. An independent investigation by energy-dispersive X-ray analysis (EDX) confirmed that these protrusions are dominantly composed of Cu.

3.2.2. XPS depth profiles

Fig. 4 reports XPS depth profiles measured through the chromate conversion coatings formed on the two samples being considered here (i.e. one was just mechanically polished in the pre-treatment, while the other also received the acid etch). These signals represent sums over the different chemical states for each element. Three main regions are apparent in the depth profiles: region I covers the topmost surface region of the coating, II spans the main part of the coating, while III refers to the transition region from coating to alloy matrix. Significant carbon is apparent in region I for both samples, although that has not been included in Fig. 4

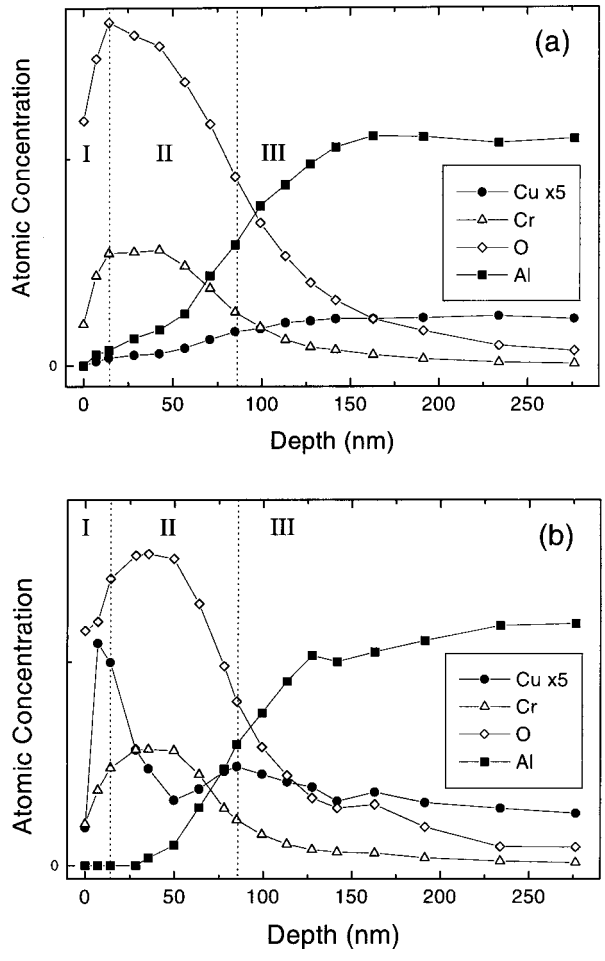

Figure 4 XPS depth profiles through chromate conversion coatings formed on Al-2024 samples after different pre-treatments: (a) mechanical polish only, and (b) subsequent 30 s etch in HF-H_2SO_4 solution.

since this component arises purely from air-borne surface contamination. The elemental distributions for Cr, Al and O are similar for both samples, but the Cu distributions are different. Thus region I for the acid-etched sample (Fig. 4b) shows enhanced Cu signals (i.e. compared with the bulk signal), whereas nothing comparable is apparent for the sample which just received a mechanical polish in the pre-treatment stage (Fig. 4a). These observations are fully consistent with the TEM and EDX observations noted above.

XPS binding energies measured for Cu, Cr and O during the depth profiling are summarized in Table I. The Cu is believed to be in metallic form for region I of both samples, although the relative amounts are quite different as seen in Fig. 4. The increase in Cu $2p_{3/2}$ binding energy with depth below the surface may indicate that the Cu is present in an oxidized state. However, the spectra do not manifest the shake-up satellites shown by CuO [24], which suggests that the Cu in the chromate coating is not well modelled by this oxide. Another possibility is that the Cu is alloyed, perhaps in cluster form [25]. In any event, this modified Cu form appears immediately below the surface for the sample that had just mechanical polishing in the pre-treatment. By contrast, this change occurs deeper below the surface for the sample that was acid etched.

The chemical state of Cr appears to vary with depth for both chromate coatings. In region I, two chemical

TABLE I Binding energies (eV) observed during depth profiling through the two different coated samples

Mechanical polishing only in pre-treatment						
Depth (nm)	Cu $2p_{3/2}$	Cr $2p_{3/2}$			O 1s	
7	932.6	578.5		576.8	530.4	532.6
35	933.2		576.9		530.5	532.6
70	933.4		576.6		530.7	532.6
84	933.4	576.8		574.3	530.8	532.5
Acid etching in pre-treatment						
Depth (nm)	Cu $2p_{3/2}$	Cr $2p_{3/2}$			O 1s	
7	932.7	579.2		577.0	530.5	532.8
35	932.7		577.0		530.4	532.3
70	933.2		576.9		530.7	532.4
84	933.4	576.8		574.3	530.8	532.5

states are identified by XPS. They have similar proportions (20%–25% Cr(VI), 80%–75% Cr(III)) for the two samples, and in both cases it is clear that the main part of the coating (i.e. region II) corresponds dominantly to Cr(III). As the alloy interface is approached (i.e. region III), a small amount of Cr(0) is apparent in both cases, although this may be ion-beam induced [26]. The depth profiling information for O 1s indicates the presence of both O^{2-} (binding energy expected close to 530.2 eV) and OH^{-} (532.0 eV) [5] in the different regions for both samples. In region I the oxide contribution is about 80% for both samples, and this decreases to 70% after the 60 min sputtering time. The trend of increasing hydroxide with depth has also been reported in other work [5]. Overall, observations for depth profiling in this study are broadly consistent with previous reports that the chromating process, as carried out here, basically yields a coating of hydrated Cr(III) oxide, and that the reduction from Cr(VI) to Cr(III) is accompanied by oxidation in the metallic substrate [4, 5, 11].

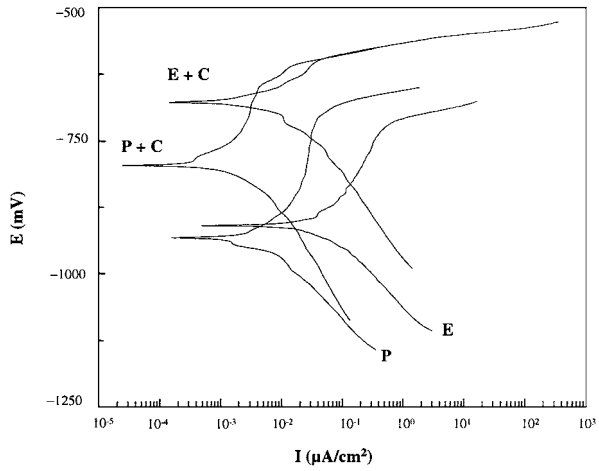

Figure 5 Polarization curves measured for Al-2024 samples after mechanical polishing (P) and acid etching (E) in pre-treatment, as well as after forming chromate conversion coatings (C) on the pre-treated surfaces as described in text.

3.2.3. Corrosion behaviours

The existence of a modified alloy layer immediately beneath the oxide film, as well as the incorporation of Cu^{2+} ions into the chromate coating on the Al-2024 alloy, may in general be expected to affect properties. In order to assess effects on corrosion behaviour resulting from the different pre-treatments, polarization measurements and immersion corrosion tests were carried out in the 3.5% NaCl solution at 20°C.

Fig. 5 shows electrochemical polarization curves measured for chromate coatings on the differently pretreated samples. A comparison is also made with the corresponding uncoated samples. In each case, the current density (which should increase with corrosion rate) was estimated from a Tafel plot by extrapolating the cathodic branch to the extrapolated anodic branch. For the uncoated samples, that which received just a mechanical polish in the pre-treatment revealed decreased current density ($0.02\ \mu Acm^{-2}$) compared with the acid-etched sample ($0.3\ \mu Acm^{-2}$). The current densities for the coated samples are much lower, but differences are still detected between the samples. Specifically, the current density for the sample which was coated after acid etching ($8.9 \times 10^{-3}\ \mu Acm^{-2}$) is higher than that for the sample where the coating was applied directly after the mechanical polish ($5.3 \times 10^{-3}\ \mu Acm^{-2}$). The former corresponds to a higher corrosion rate, and that in turn should result from differences in the structure and composition of the coatings.

Fig. 6 compares SEM micrographs obtained from the chromated samples before and after a 24 h immersion in the 3.5% NaCl solution. No changes in the alloy matrix or the second-phase particles are apparent for the sample that received just the mechanical polish in the pre-treatment (compare Fig. 6a and b) whereas, for the sample that was coated after acid etching, substantial corrosion is revealed after the immersion (compare Fig. 6c and d). Initially, the latter coated surface is relatively rough although, after immersion, there is evidence for deposition adjacent to cathodic second-phase particles, and this results in formation of a flatter surface.

4. Discussion

The corrosion behaviours of the two chromate-coated samples compared in this work inevitably depend on the details of the composition and structure of the coatings. The Al-2024 sample that was acid-etched in the pre-treatment corrodes more readily than that which just received the mechanical polish. Associated with this difference is the different distributions of Cu in the two coated samples. As noted above, the acid-etched sample shows evidence for Cu enrichment at the alloy-coating

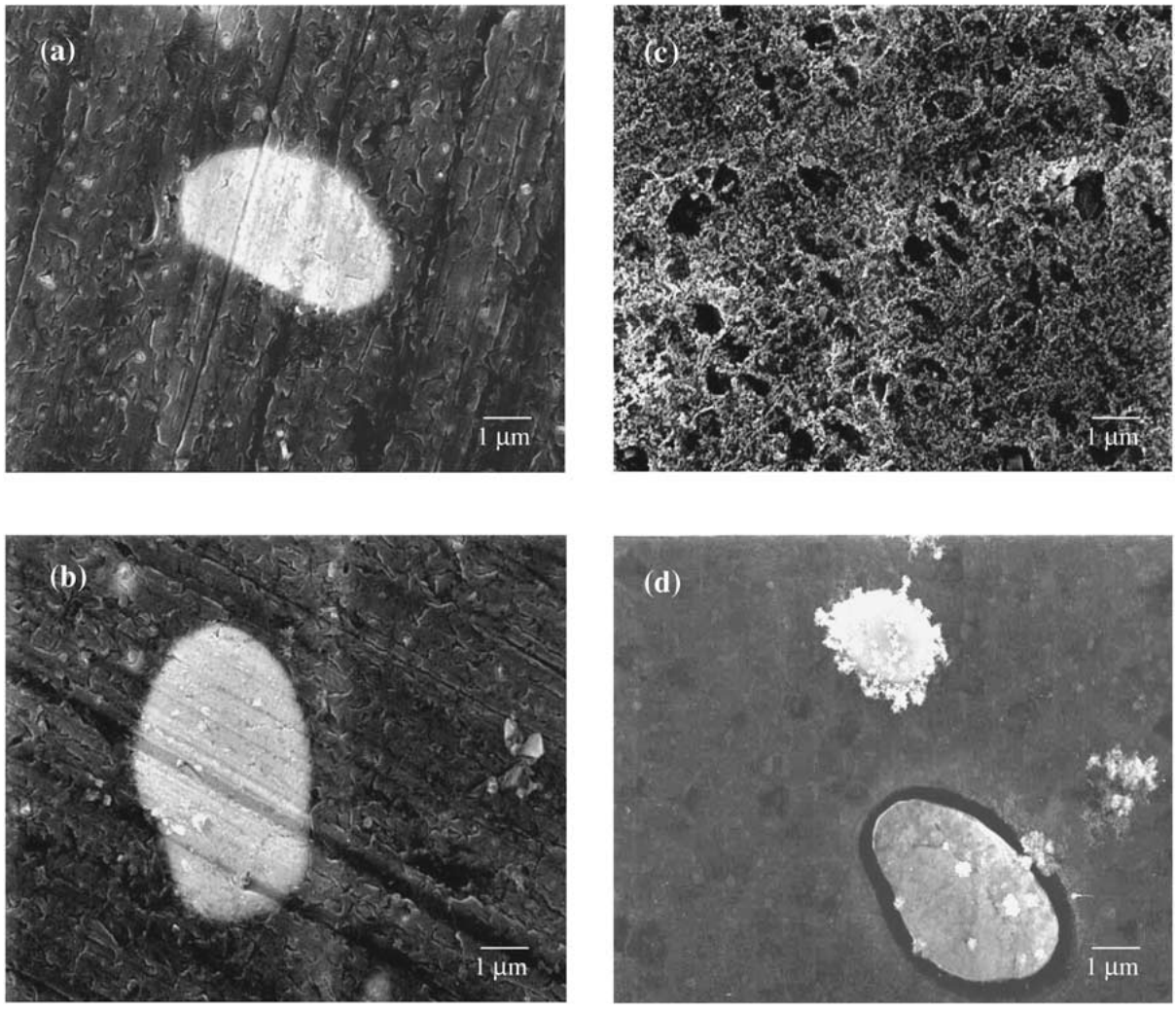

Figure 6 SEM images of chromate-coated Al-2024 samples before and after immersion in 3.5% NaCl solution for 24 h: (a) coated sample whose pre-treatment involved mechanical polishing only; (b) as (a) but after immersion test; (c) coated sample whose pre-treatment included the acid etch; (d) as (c) but after immersion test.

interface, Cu incorporation into the chromated coating, as well as a migration and Cu redeposition from solution on to the top surface. These aspects are discussed further in the following.

4.1. Interfacial enrichment of copper after pre-treatment

Observations by XPS and TEM reported above clearly indicate that the different pre-treatments markedly affect the initial composition of the Al-2024 surface region. Mechanical polishing appears mainly to introduce changes in surface morphology (e.g. generation of scratches), while acid etching involves oxidation which can lead to changes in composition. The interfacial enrichment of alloying elements in aluminum alloys has recently received considerable attention due to its theoretical and practical importance [15, 16, 27]. For example, it has been concluded that the extent of enrichment of an alloying element can be predicted by comparative values of the Gibbs free energy of formation per equivalent of oxide ($\Delta G^\circ/n$) relative to that of aluminum. $\Delta G^\circ/n$ values for both CuO (-64.9 kJmol^{-1}) and Cu_2O (-73.0 kJmol^{-1}) are greater than that of Al_2O_3 (-263.7 kJmol^{-1}), and on this basis Cu is expected to show a significant enrichment at the surface of an Al-Cu alloy in an oxidizing environment [27]. This prediction is consistent with observations made in the present work although, as noted above, XPS is ambiguous as to whether the Cu in the enriched layer, formed by the acid-etch, is in the metallic or Cu_2O forms (the Cu 2p binding energies are very similar).

XPS studies of the mechanically polished 2024-alloy surface indicate a surface composition similar to that in the bulk ($\sim$4 wt% Cu). The amount of Cu in the enriched layer after acid etching increases by an order of magnitude, and similar observations have been made by RBS [28]. The structure of the enriched layer may also be important for understanding the effect of this layer on a subsequent oxidation. At the resolution available in the TEM used in this work, no significant discrete features are evident within the Cu-enriched regions, which appear as uniformly dark bands at the alloy-to-oxide interfaces. However, the formation of Al_2Au nanocrystals within a Au-enriched layer (3–5 nm thick) for an Al–Au (0.4at%) alloy has been reported by high-resolution TEM [25]. The growth of Cu-rich clusters within the enriched layers in the present context is expected to encourage oxidation at these sites.

4.2. Migration and redeposition of copper at coatings

XPS depth profiles through the chromated coatings on the differently pre-treated Al-2024 samples show different behaviours. For the initial surface that was just mechanically polished only low levels of Cu are present in the coating (i.e. at concentrations less than that for the bulk alloy). By contrast, the coating on the initial surface that received the acid etch contains more Cu, and information from the depth profile is fully consistent with Cu migration from the alloy interface and through the coated region. Further, the respective distributions show that the Cu migration through the chromated film is faster than that for Al, and this is consistent with observations for the anodizing process [15]. The depth profile in Fig. 4b detects a slight accumulation of Cu at the chromate-to-alloy interface; this may relate to the dark band (3 nm thickness) observed by TEM (Fig. 3b), and hence support the view that the Cu enriched layer is maintained during the chromating process.

Whatever the precise chemical state of the Cu in the coating, the dichromate can oxidize further at the electrolyte interface so that Cu^{2+} ions pass into solution. The evidence reported here by TEM, EDX and XPS, for the sample which had initially been acid etched during the pre-treatment, is consistent with local conditions at the liquid interface building up to allow Cu redeposition at particular sites on the coated surface. The mechanistic details of this process remain unknown, but the protruding Cu-rich regions (Fig. 3b) produced are expected to act as local cathodic sites and facilitate corrosion, and this contrasts with the situation for the other chromated sample which did not receive an acid etch in the pre-treatment prior to the coating.

5. Concluding remarks

Although other work has previously shown that different pre-treatments can directly influence the compositions at surface regions of Al alloys, this work highlights an interesting feature that this initial enrichment can affect the composition and properties of a subsequent conversion coating. That opens a significant question of whether control of surface enrichment can aid the design of appropriate coatings for corrosion protection. The present study for chromate coating was undertaken in order to provide a reference for comparison with parallel work being done on alternative non-chromated coatings. Inevitably, other coating processes may be affected differently by the enrichment effects. Thus observations from this laboratory for zinc phosphate coatings formed on Al-2024 alloy has shown that the surface enrichment of Cu in appropriate amounts can be used to increase corrosion protection [20], and this contrasts with the situation reported here.

Acknowledgements

The authors thank the Natural Sciences and Engineering Research Council of Canada and the Department of National Defence for support of this work. We are also grateful to Prof. D. Tromans for use of his Solartron potentiostat and Mr. Andre Wong for the TEM service.

References

1. S. WERNICK, R. PINNER and P. G. SHEASBY, "The Surface Treatment and Finishing of Aluminum Alloys" (Finishing Publications, Teddingdon, Middlesex,1987) Ch. 5.
2. S. M. COHEN, *Corrosion* **51** (1995) 71.
3. J. A. TREVERTON and N. C. DAVIES, *Surf. Interface Anal.* **3** (1981) 194.
4. K. ASAMI, M. OKI, G. E. THOMPSON, G. C. WOOD and V. ASHWORTH, *Electrochimica Acta* **32** (1987) 337.
5. A. E. HUGHES and R. J. TAYLOR, *Surf. Interface Anal.* **25** (1997) 223.
6. A. C. MILLER and G. M. MALOUT, *Appl. Surf. Sci.* **2** (1979) 416.
7. P. L. HAGANS and C. M. HAAS, *Surf. Interface Anal.* **21** (1994) 65.
8. M. F. A. RABBO, J. A. RICHARDSON and G. C. WOOD, *Corrosion Sci.* **18** (1978) 117.
9. Y. ZUZHAN, N. HONGBING and C. GUANSHEN, in "Aluminum Surface Treatment Technology," edited by R. S. Alwitt and G. E. Thompson (The Electrochemical Society, Pennington, NJ, 1986) p. 216.
10. F. W. LYTLE, G. L. BIBBINS, K. Y. BLOHOWIAK, R. B. GREEGOR, R. E. SMITH and G. D. TUSS, *Corrosion Sci.* **37** (1995) 349.
11. J. K. HAWKINS, H. S. ISAACS, S. M. HEALD, J. TRANQUADA, G. E. THOMPSON and G. C. WOOD, *ibid.* **27** (1987) 391.
12. G. M. BROWN, K. SHIMIZU, K. KOBAYASHI, G. E. THOMPSON and G. C. WOOD, *ibid.* **34** (1993) 1045.
13. *Idem.*, *ibid.* **33** (1992) 1371.
14. *Idem.*, *ibid.* **35** (1993) 253.
15. H. HABAZAKI, K. SHIMIZU, M. A. PAEZ, P. SKELDON, G. E. THOMPSON, G. C. WOOD and X. ZHOU, *Surf. Interface Anal.* **23** (1995) 892.
16. M. A. PAEZ, T. M. FOONG, C. T. NI, G. E. THOMPSON, K. SHIMIZU, H. HABAZAKI, P. SKELDON and G. C. WOOD, *Corrosion Sci.* **38** (1996) 59.
17. H. H. STREHBLOW and C. J. DOHERTY, *J. Electrochem. Soc.* **125** (1978) 30.
18. H. H. STREHBLOW, C. M. MELLIOR-SMITH and W. AUGUSTYNIAK, *ibid.* **125** (1978) 915.
19. X. WU and K. HEBERT, *ibid.* **143** (1996) 83.
20. X. SUN, W. H. KOK, K. C. WONG, R. LI, K. A. R. MITCHELL and T. FOSTER, *ATB Metallurgie* **40–41** (2000/2001) 503.
21. P. C. WONG, Y. S. LI, M. Y. ZHOU and K. A. R. MITCHELL, *Appl. Surf. Sci.* **89** (1995) 255.
22. R. C. FURNEAUX, G. E. THOMPSON and G. C. WOOD, *Corrosion Sci.* **18** (1978) 853.
23. C. D. WAGNER, in "Practical Surface Analysis," edited by D. Briggs and M. P. Seah (John Wiley, Chichester, 1990), p. 595.
24. J. HABER, T. MACHEJ, L. UNGIER and J. ZIOLKOWSKI, *J. Solid State Chem.* **25** (1978) 207.
25. H. HABAZAKI, K. SHIMIZU, P. SKELDON, G. E. THOMPSON and G. C. WOOD, *Phil. Mag.* **B73** (1996) 445.
26. S. HOFMANN, in "Practical Surface Analysis," edited by D. Briggs and M. P. Seah (John Wiley, Chichester, 1990) p. 143.
27. H. HABAZAKI, K. SHIMIZU, P. SKELDON, G. E. THOMPSON, G. C. WOOD and X. ZHOU, *Trans. Institute Metal Finishing* **75** (1997) 18.
28. H. HABAZAKI, X. ZHOU, K. SHIMIZU, P. SKELDON, G. E. THOMPSON and G. C. WOOD, *Electrochimica Acta* **42** (1997) 2627.

Received 8 June
and accepted 20 December 2000